Geothermal Reservoir Identification in Way Ratai Area Based on Gravity Data Analysis

M Sarkowi, R C Wibowo*, and Karyanto

Geophysical Engineering, Engineering Faculty, Universitas Lampung, Indonesia

*Email: rahmat.caturwibowo@eng.unila.ac.id

Abstract. Gravity research in the Way Ratai geothermal prospect area was conducted to determine geothermal reservoirs, heat sources, and the structure of the geothermal reservoir. The research carried out includes 3D inversion modeling of gravity data. The Bouguer anomaly in the study area has 50 mGal to 120 mGal with low anomalies located in the southeast (Ketang and Kelagian), Northeast (Gedong Air, Sungai Langka, Gunung Betung) areas, and in the Pesawaran mountain area. The high anomaly is in Merawan – Hanuberak – Padang Cermin, Sumbersari and Kaliawi. The horizontal gravity gradient map analysis shows a pattern of fault structure trending northwest-southeast and southwest-northeast, according to the main fault structure in the area. 3D inversion modeling obtains a density distribution between 1.8 g/cc to 3 g/cc with a low-density distribution in the south, Mount Pesawaran/Ratai, Gunung Betung, and Sidoharum. The location of the manifestation is 9 km southeast of the Mount Ratai/Pesawaran summit. The existence of geothermal reservoirs is estimated to be in the Lubuk Badak and Miwung Hills areas which are located between the peaks of Mount Ratai/Pesawaran and geothermal manifestations. This is supported by the low-density distribution in the area and the resistivity map from audio-magnetotelluric data.

1. Introduction

The Way Ratai Geothermal area is located in a volcanic complex which has two volcanic cones side by side, namely Mount Pesawaran in the southwest and Mount Betung in the northeast. Mount Pesawaran has peaks, namely: Pematang Petai Peak, Kambing Neck Peak and, the highest, Tugu/Ratai peak (Figure 1). Mount Pesawaran and Mount Betung are part of the many volcanoes on Sumatra that form a model of the volcanic hydrothermal system or liquid-dominated high standing terrain [1,2].

The Way Ratai geothermal prospect area is geographically located in Pesawaran Regency and Bandar Lampung City. Several studies have been conducted to determine the geothermal system in the Way Ratai area. This area has an estimated reserve of 105 MW [3]. Magnetic research around the Way Ratai geothermal manifestation found a low magnetic anomaly associated with manifestations in the area. The area is estimated to be an outflow zone [4].

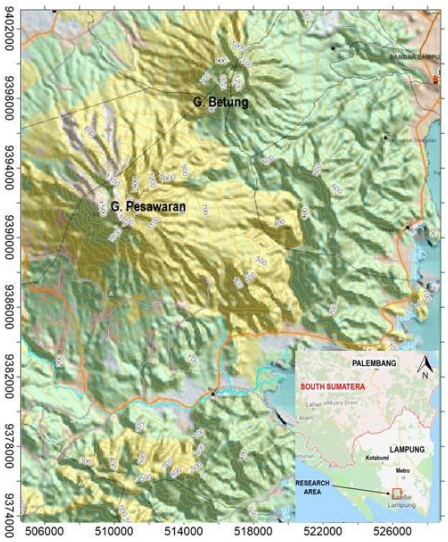

Figure 1. Research area location, Way Ratai geothermal

Radon's research shows that geothermal manifestations in the Way Ratai geothermal area (Kali Asin – Bambu Kuning – Padok – Kali Tigas) are correlated with the presence of SW-NE trending faults [5]. Taufiq conducted a gravity study only in the Way Ratai geothermal manifestation area, which found a graben to the north of the geothermal manifestation [6]. The Way Ratai geothermal manifestation area has a reasonably high temperature, which is between 85^{o}C – 98^{o}C. Measurement of the thermal conductivity of the area around the manifestation to get the value of thermal conductivity: 0.056 to 0.644 W/mK. This thermal conductivity value is influenced by geological structures such as the presence of faults, the presence of alteration zones, and the presence of manifestations in the area [7].

Research that previous researchers have carried out has concentrated on the area around the geothermal manifestation. In contrast, research in the north, between Mount Pesawaran and the manifestation area, has not been carried out. For this reason, in this study, processing and analysis of gravity data will be carried out in the Way Ratai geothermal prospect area, which covers 12 x 15 km and includes the area of Mount Pesawaran, Mount Betung, and geothermal manifestation areas. This study aims to obtain the structure and location of the geothermal reservoir prospect area and the heat source of the Way Ratai geothermal system.

Rock dominates the geology of the study area from young volcanoes (Qhv) both from Mount Pesawaran/ Ratai and Mount Betung, which consist of lava rock (andesite-basalt), breccia, and tuff (Figure 2). Stratigraphy of the Way Ratai geothermal field is grouped into four groups [8], namely:

a. Tertiary rocks, sedimentary rocks from the Ratai Formation, are composed of conglomerates, sandstones, breccias lava, and claystones sometimes associated with andesite tuff, which are scattered on the south-southwest side.
b. Pre-Eruption Volcanic Rocks of Mount Betung and Ratai. Groups of volcanic rocks from old to young are volcanic Gebang rock (GV), ignimbrite Gebang rock (GI), lava flow Gebang rock (GL), debris deposit (ED), and Banjarmeger volcanic rock (BV).
c. Volcanic Rocks Eruption of Mount Betung and Ratai. Quaternary volcanic rocks erupted into two eruption sources, namely the eruption of Mount Betung and Ratai at the base of the Gebang Caldera.
d. Surface Deposits, which consist of Lava (LH) and Alluvium Deposits.

Normal fault structures dominate the fault structure in the Way Ratai geothermal field and its surroundings with SE-NW and NE-SW directions. The study area is also characterized by the main trending lineaments NE-SW and SE-NW. Lineaments are present quite a lot, especially in the west, southwest, south, and slightly in the center of the study area. Geothermal manifestations are scattered in

the southeastern part of the study area, namely: Kali Tiga (85°C), Padok (96°C), Bambu Kuning (90°C), Margodadi (98°C), Way Asin (85°C).

2. Method

The data used is satellite gravity data of 238 gravity points spread over Mount Pesawaran - Mount Betung and its surroundings with an area of 12 km x 15 km [9]. Gravity data is carried out by Boguer correction so that the Bouguer anomaly is obtained. Spectrum analysis was carried out on several paths so that the average depth of the regional Bouguer anomaly was carried out. The power spectrum of the Bouguer anomaly is carried out by transforming the Fourier gravity data into the frequency domain [10]:

$$F(g) = 2\pi\gamma m \frac{e^{|k|(z_0 - z_1)}}{|k|} \tag{1}$$

The energy spectrum of the equation is:

$$E(k) = \frac{4\pi^2\gamma^2\rho^2}{|k|^2} e^{-2|k|z} \tag{2}$$

$$\log E(k) = \log(4\pi^2\gamma^2\rho^2) - 2|k|z - 2\log|k| \tag{3}$$

$$\log E(k) = \log A - 2|k|z \tag{4}$$

where: Z_0 (depth of point measurement), Z_1 (center of mass depth) $Z_1 > Z_0$, $k = 2\pi/\lambda$ ((wave number), λ (wavelength), g (gravity anomaly), and ρ (density).

From these equations, it can be determined the wavelength and depth of anomaly objects. First-order horizontal gravity gradient analysis ($FHDx = \frac{\Delta g}{\Delta x}$, $FHDy = \frac{\Delta g}{\Delta y}$, $SFHD = FHDx + FHDy$) [11,12] and the second order ($SHDx = \frac{\Delta^2 g}{\Delta x^2}$, $SHDy = \frac{\Delta^2 g}{\Delta y^2}$, $SSHD = SHDx + SHDy$) [13-15] carried out to obtain fault structures/intrusions/lithological boundaries as well as sources of anomalies originating close to the surface [10-16]. Gradient analysis correlates gravity gradient with geological and geochemical maps to obtain fault structure patterns or lithological boundaries in the area [16].

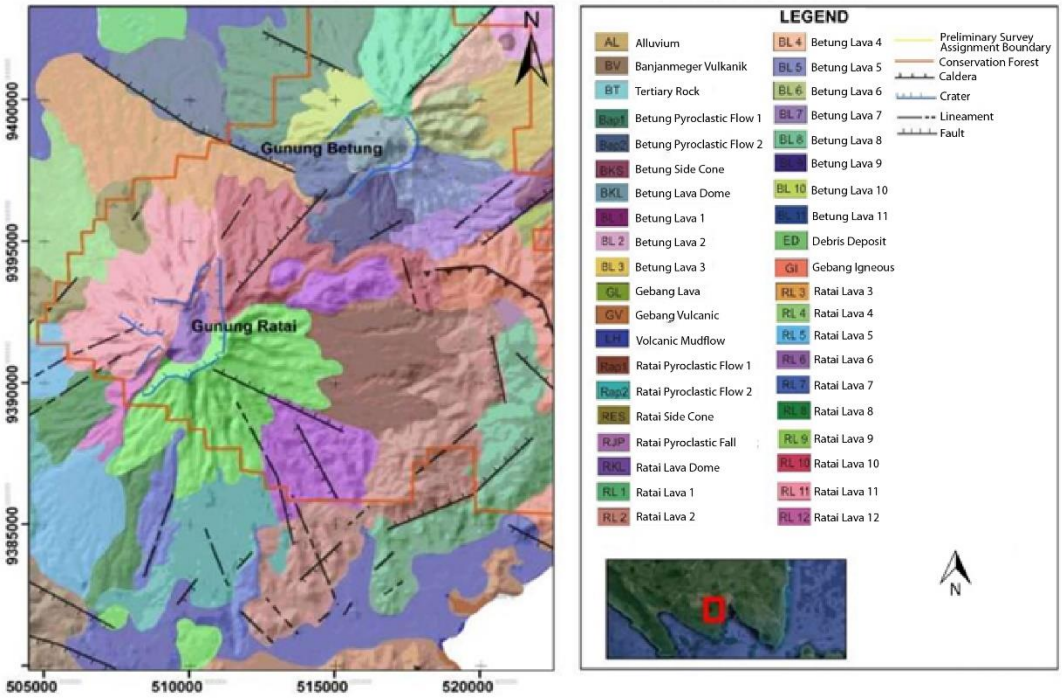

Figure 2. Research area location, Way Ratai geothermal

Bouguer anomaly 3D inversion modeling was conducted to obtain a subsurface density distribution model [17,18] using the GRAV3D 2.0 program [19]. Based on the density distribution model and correlation with geological, geochemical, and other geophysical data are obtained, the fault structure, geothermal reservoir, and heat source of the Way Ratai geothermal system.

3. Results and Discussion

The Bouguer anomaly in the study area has a value of 45 mGal to 120 mGal, with high anomalies in the western part (Merawan, Sidomulyo, Sentongan, Bunut, Hanuberak, and Padang Cermin areas which correlate with Tertiary rocks), Malawi, Sumbersari, and Sanggi areas. Low anomalies are in Mount Pesawaran, Mount Betung, and the southeastern part of the study area (Figure 3).

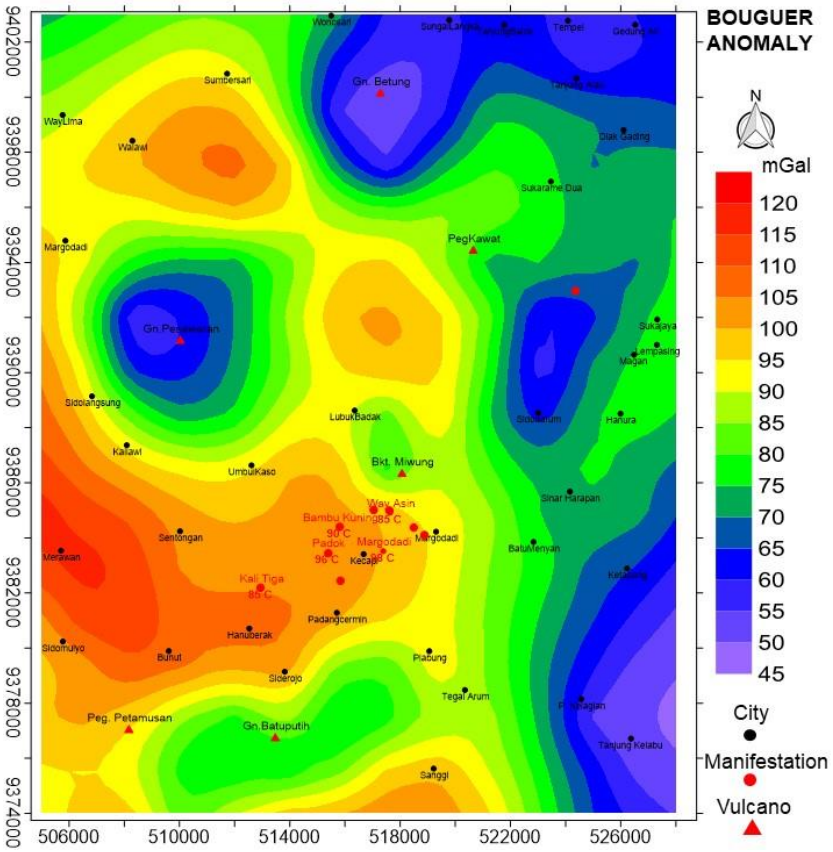

Figure 3. Bouguer anomaly map of the research area and geothermal manifestations, Mount Pesawaran, and Mount Betung location

Spectrum analysis was carried out by making a cross-sectional trajectory of the Bouguer anomaly to get the depth of the regional anomaly. The spectrum analysis results for 6 cross-sectional paths of the Bouguer anomaly with an average depth of 3,293 meters (Figure 4). The depth of this regional anomaly correlates with the average depth of the basement rocks in the area.

3.1. Bouguer anomaly horizontal gradient

To support the Bouguer anomaly analysis in identifying fault structures, lithological boundaries and to generate shallow effect anomalies, a vertical gradient analysis of the Bouguer anomaly was carried out. Theoretically, the horizontal gradient method of the Bouguer anomaly is the derivative of the Bouguer anomaly for the horizontal direction, which can be written as first-order horizontal gradient x-direction = $FHDx = \frac{\Delta g}{\Delta x}$ and first-order horizontal gradient y-direction = $FHDy = \frac{\Delta g}{\Delta y}$, while second-order horizontal gradient x-direction = $SHDx = \frac{\Delta^2 g}{\Delta x^2}$ and second-order horizontal gradient y-direction = $SHDy = \frac{\Delta^2 g}{\Delta y^2}$.

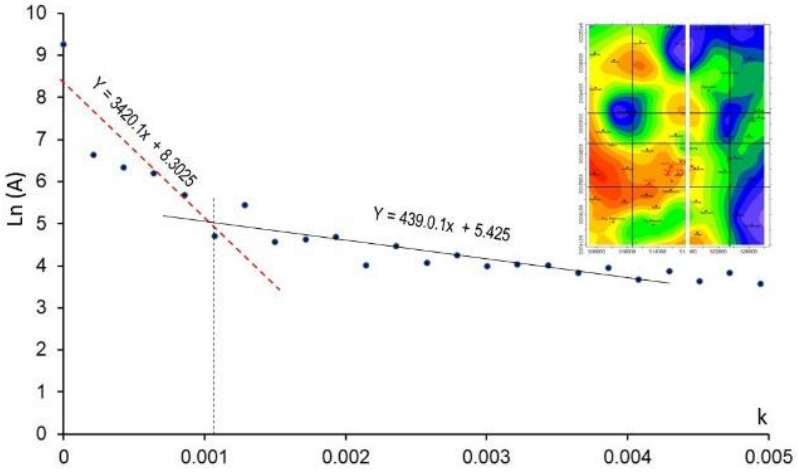

Figure 4. Spectrum analysis of the West-East trajectory, which obtained the regional anomaly boundary and residual 3,420.1 m

In general, fault structures, intrusions, lithological boundaries, and boundary models of anomaly objects are not always in the x or y-direction. The sum of the horizontal gradients in the x and y directions is used in the horizontal gradient analysis. That analysis of the sum of SFHD ($SFHD = FHDx + FHDy$) and the sum of SSHD ($SSHD = SHDx + SHDy$) are applying in this study.

Horizontal gradient analysis of the Bouguer anomaly is carried out to reveal anomalies that originate close to the surface and also to find out: boundaries of density changes, lithological boundaries, intrusions, presence of faults, and others [12,15,20]. The first-order and second-order horizontal gradient analysis in the Way Ratai geothermal area was carried out to obtain the presence of fault structures or lithological rock boundaries. The analysis is carried out by correlation or comparison with geological data and geothermal manifestations. The first-order horizontal gradient map of the study area is shown in Figure 5. The presence of a fault, intrusion, lithological boundary, and density change limit is indicated by the maximum or minimum value of the first-order horizontal gradient anomaly map [13,21]. The contour of the horizontal gradient anomaly of the order of the Bouguer anomaly shows that there is a dominant maximum and minimum anomaly pattern with a southeast-northwest trending which indicates a structure that has a southeast-northwest trending. This structural pattern is in accordance with the pattern of the main fault structure trending southeast–northwest in the area [8].

The second-order horizontal gradient map of the Bouguer anomaly in the Way Ratai geothermal area is shown in Figure 6. The presence of fault structures, lithological boundaries, intrusion structures, caldera, and density changes limits are shown by the horizontal gradient value of order-2 Bouguer anomaly = 0 (zero) [19]. Analysis of the presence of fault structures, lithological boundaries, intrusion structures, calderas, and density changes boundaries is carried out by analyzing the contours of the horizontal gradient anomaly of order 2 Bouguer anomaly with a value of 0 (zero). The second-order horizontal gradient anomaly contour of the Bouguer anomaly in the Way Ratai geothermal prospect area has a dominant 0 anomalous contour pattern with the direction of southeast-northwest, which indicates a fault with a direction southeast-northwest in the area. This follows the structural pattern of the main fault structure trending southeast-northwest in the area [8]. Besides that, there is also a horizontal gradient anomaly pattern of second-order Bouguer anomaly with a zero value trending southwest-northeast, which indicates a fault with a southeast-northwest trending in the area following the geological structure in the area [8].

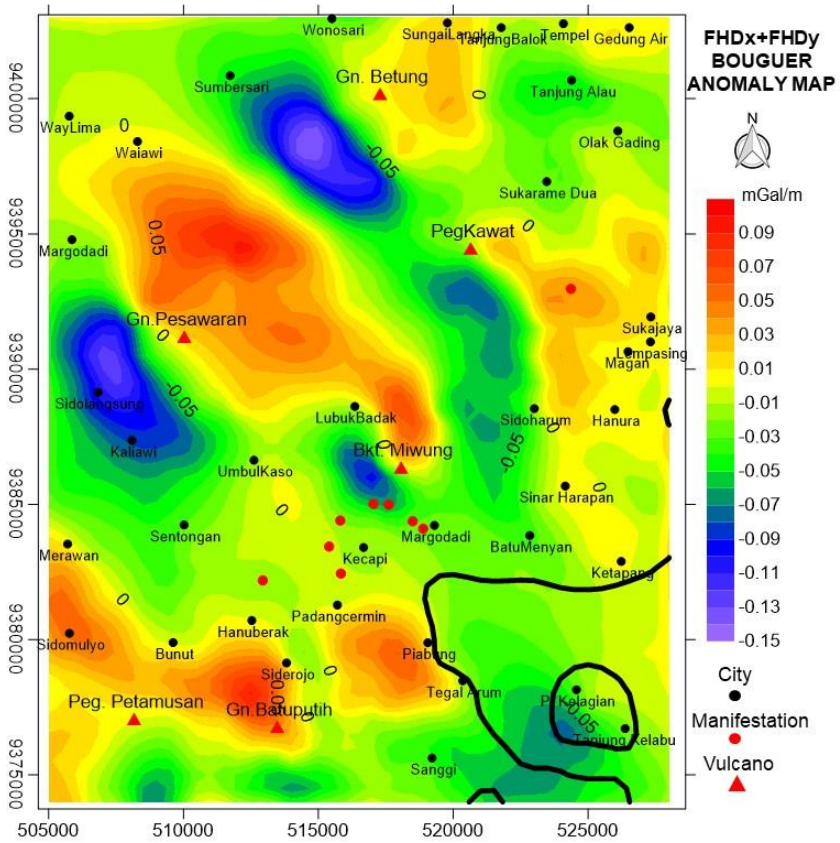

Figure 5. The first order gradient map of the Bouguer anomaly of the research area and the location of geothermal manifestations and Mount Pesawaran and Mount Betung

The second-order horizontal gradient contour of the Bouguer anomaly with a value of 0 (zero) which forms a closing closure around Mount Pesawaran and Mount Betung, is probably related to the lithology of the volcanic products of the mountain and the presence of magmatic rock under Mount Pesawaran and Mount Betung.

3.2. 3D modeling

Modeling the 3D inversion of the Bouguer anomaly is done to get a subsurface structure model of the Way Ratai geothermal field. The equation used and the calculation of the 3D inversion modeling is the subsurface model approach composed of prisms with the number of adjusting to measurement area, data grid, thickness, and depth of objects. Calculation of the gravity response of each prism block using the Plouff equation [22]:

$$g = G\Delta\rho\sum_{i=1}^{2}\sum_{j=1}^{2}\sum_{k=1}^{2}\mu_{ijk}\left[z_k \arctan\frac{x_i y_i}{z_k R_{ijk}} - x_i \log\left(R_{ijk}+y_i\right) - y_i \log\left(R_{ijk}+x_i\right)\right] \quad (5)$$

where: $R_{ijk} = \sqrt{x_i^2 + y_j^2 + z_k^2}$ and $\mu_{ijk} = (-1)^i (-1)^j (-1)^k$

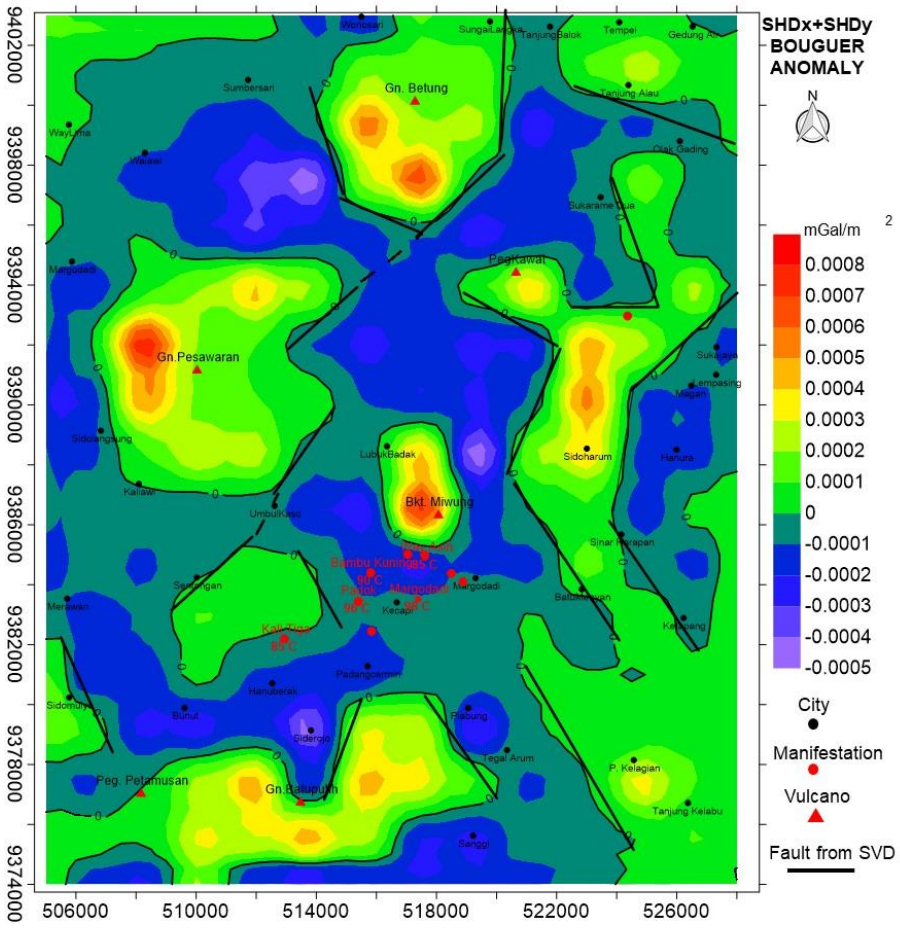

Figure 6. Second-order gradient map of the Bouguer anomaly and geothermal manifestations, Mount Pesawaran and Mount Betung location

The 3D inversion modeling of the Bouguer anomaly using the 3D Grav program is carried out by creating a subsurface object model composed of a box model with specific dimensions and depths. The box model is arranged in a mesh with the same dimensions as the area of the Bouguer anomaly data. The depth is adjusted according to geological information and depth results from spectrum analysis. Meanwhile, the input is the Bouguer anomaly data grid and the topographic data grid. The results of the 3D inversion modeling are shown in Figure 7.

The density distribution model from the 3D inversion model obtained a density value between 1.8 g/cc to 2.9 g/cc. To obtain a detailed model of the subsurface density distribution, slicing is done either horizontally or vertically so that the distribution of the subsurface density model can be known in detail [23]. To interpret the model, comparisons are made with geological data and other geophysical data [24,25]. The cross-sectional model of the subsurface density distribution in the S–N direction correlates manifestations. The fault structure model identified from the horizontal gradient analysis of first-order and second-order is shown in Figure 8. In this path, there are low-density models in the south-central and northern parts. The presence of geothermal manifestations in the middle that comes out through the fault line indicates a geothermal reservoir near the area. The possibility of a low-density model in the middle is related to the presence of a geothermal reservoir.

The cross-sectional model of the subsurface density distribution in the NW–SE direction, which correlates with the fault structure model identified from the first-order and second-order horizontal gradient analysis, is shown in Figure 9. Faults in this path limit low-density models on the left, middle, and right sides. The low density on the left under Mount Pesawaran is probably the result of former volcanic activity. In contrast, the high density on the left and under Mount Pesawaran may be related to the remaining magma that can function as a heat source for the geothermal system in the area. The low

density in the middle, precisely in the Lubuk Badak and Miwung hills, can be interpreted as a geothermal reservoir supported by geothermal manifestations in the south of the area.

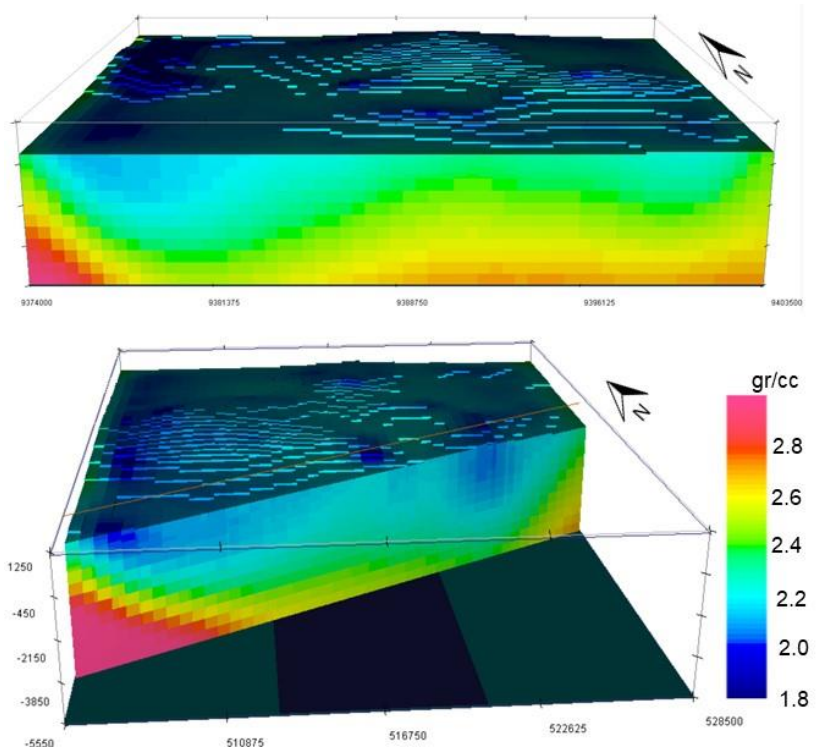

Figure 7. The subsurface density distribution model results from the 3D inversion modeling of the Bouguer anomaly in the Way Ratai geothermal area

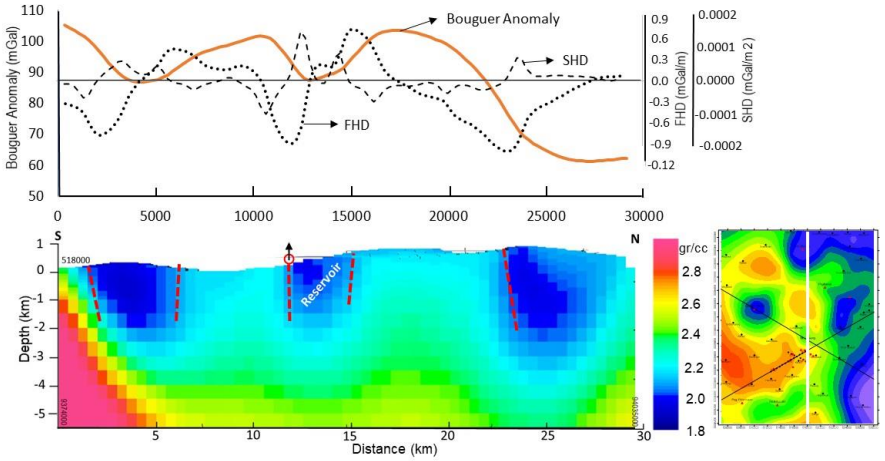

Figure 8. The cross-sectional model of the subsurface density distribution in the S–N direction correlates with manifestations. The fault structure model was identified from the analysis of horizontal gradients of first-order and second-order

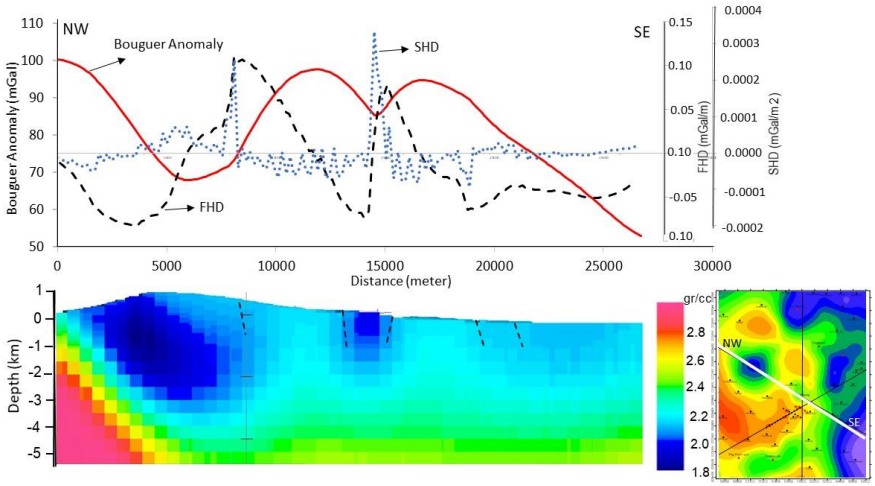

Figure 9. The cross-sectional model of the subsurface density distribution in the NW–SE direction is correlated with the fault structure model identified from the analysis of horizontal gradients of first-order and second-order

The cross-sectional model of the subsurface density distribution of the SW–NE direction correlated with the manifestation, the fault structure model identified from the first and second order horizontal gradient analysis, and the resistivity model of the AMT [23] is shown in Figure 10. In this path, there is a low-density model in Figure 10: the left (Bunut) and right (Sidoharum), which are limited by faults. The correlation of the density model in the middle (manifestation area) with the resistivity model from AMT shows a good correlation, namely the presence of manifestations in Padok and Kaliasin in the fault area, which is clearly illustrated from the AMT model and the gravity gradient analysis. The presence of caprock in the manifestation area indicates that underneath there is a geothermal reservoir around the manifestation area [27].

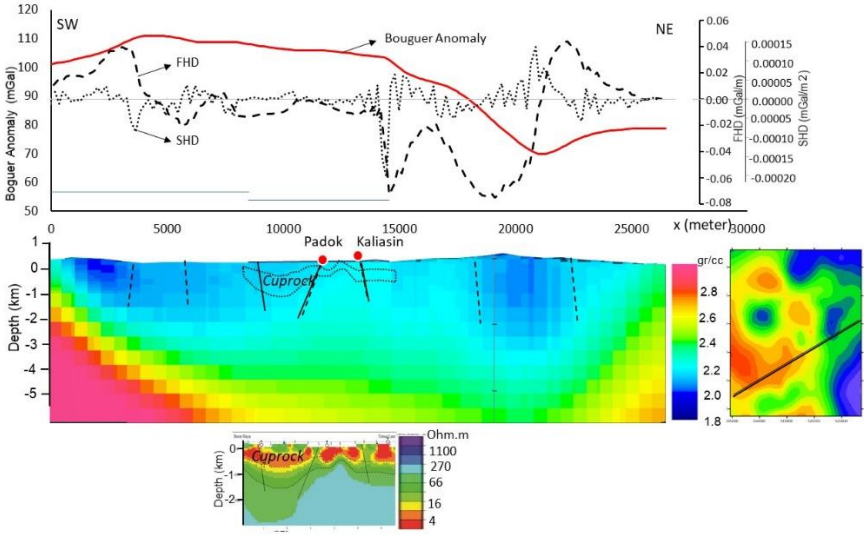

Figure 10. The cross-sectional model of the subsurface density distribution in the SW–NE direction is correlated with the resistivity model from AMT [23], the presence of manifestations, and the fault structure model identified from the horizontal gradient analysis of first-order and second-order

The cross-sectional density distribution model at a depth of 1,000 meters below MSL is correlated with contour 0 second-order horizontal gradient map, presence of manifestations, Mount Pesawaran and Mount Betung (Figure 11).

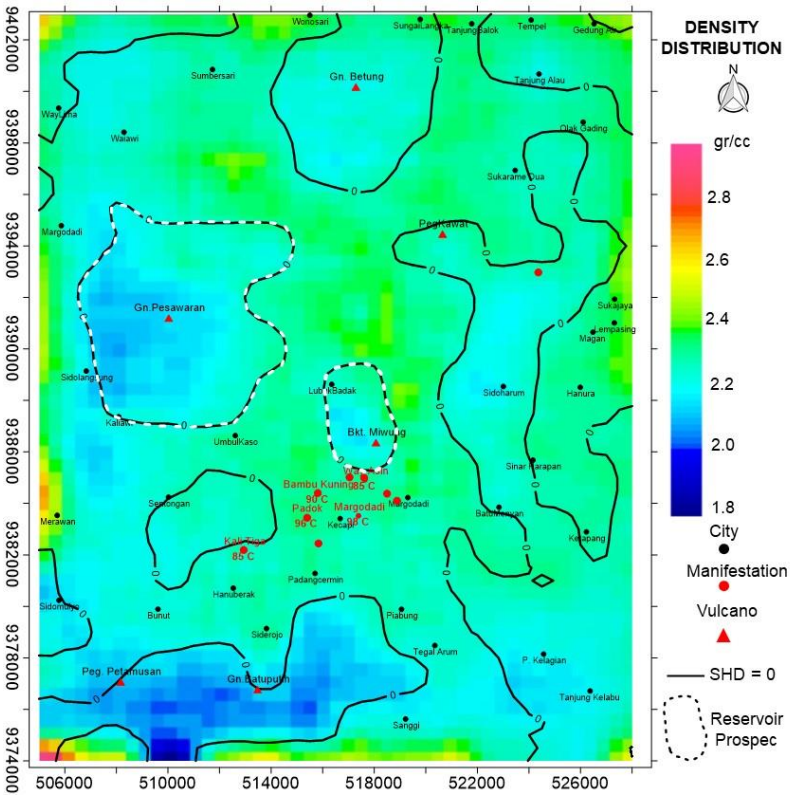

Figure 11. The cross-sectional density distribution model at a depth of 1000 meters below MSL is correlated with: contour 0 (zero) horizontal gradient map of second-order, presence of manifestations, and Mount Pesawaran and Mount Betung

The low-density distribution model (ρ < 2.2 g/cc) is located in the following areas: Gunung Pesawaran, Gunung Betung, Petamusan mountain, Mount Batuputih, Lubuk Balak, Miwung Hill, Tanjung Alu, Sidoharun and around the island of Kelagian. This low-density model is at a low-order second horizontal anomalous gradient ($SHDx + SHDy < 0$ mGal/m^2). Reservoirs in good geothermal systems generally have high porosity and permeability, and low density [24].

Based on this, areas with low density will function as good reservoirs, but not all areas with low density can function as reservoirs. The existence of a reservoir in an area is also strongly influenced by caprock, which will trap the hot fluid in the geothermal reservoir to not come out to the top. From the resistivity map, the results of AMT data processing in the area around the manifestation show a low resistivity zone which is interpreted as caprock at depths below 500 meters [23]. The caprock in the manifestation area is likely to continue to the North and Northwest.

The prospect of the Way Ratai geothermal system is a volcanic geothermal system where the heat source comes from the presence of a volcano. The heat source from the Way Ratai geothermal system may come from the Mount Pesawaran area. This is also supported by the results of the inversion modeling, which found a high density around the Mount Pesawaran area. The location of the heat source in Mount Pesawaran and the emergence of geothermal manifestations that appear in the southeast can be interpreted as that the existence of the geothermal reservoir is located between Mount Pesawaran and the manifestation area, namely in the Miwung Hills, Lubuk Badak, Umbul Kaso, and around the peaks of Mount Pesawaran. The Lubuk Badak and Bukit Miwung reservoir areas are the most prospective reservoirs of the several prospective geothermal reservoir areas. These areas have low density, and in the south, there are geothermal manifestations with high temperatures (98^{o}C).

4. Conclusion

The Bouguer anomaly in the study area has a value of 50 mGal to 120 mGal with low anomalies located in the Southeast area (Ketang and Kelagian), the Northeast area (Gedong Air, Sungai Langka, Gunung Betung), the middle area (Bukit Miwung and Lubuk Badak) and in the middle area (Bukit Miwung and Lubuk Badak). Pesawaran Mountain. The high anomaly is in Merawan – Hanuberak – Padang Cermin, Sumbersari and Kaliawi. The horizontal gravity gradient map analysis shows a pattern of fault structure trending northwest-southeast and southwest-northeast, which is following the main fault structure in the area.

The Way Ratai geothermal prospect area is a volcanic geothermal system with a heat source located on Mount Pesawaran, supported by high anomalies around the area. The existence of geothermal potential in the Way Ratai area is indicated by the presence of geothermal manifestations in the study area spread over 6 areas, namely: Kalitiga (85^{o}C), Padok (96^{o}C), Margodadi (98^{o}C), Bambu Kuning (90^{o}C), Way Asin (85^{o}C), and the other side of the island. West Sukajaya. The location of the manifestation is 9 km to the southeast of the summit of Mount Ratai/Pesawaran (heat source).

3D inversion modeling obtained a density distribution between 1.8 g/cc to 3 g/cc with a low-density distribution ($\rho < 2.2$ g/cc) located in Gunung Pesawaran, Gunung Betung, Petamusan Mountain, Mount Batuputih, Lubuk Balak, Miwung Hill, Tanjung Alu, Sidoharun and around the island of Kelagian. Based on the cross-sectional model of density distribution and horizontal gradient anomaly profile, both first-order and second-order, it is found that there is a low-density area bounded by a fault structure to the north of the manifestation. The low-density model in the Bukit Miwung and Lubuk Balak areas which are located between Mount Pesawaran and geothermal manifestations, can be interpreted as the most prospective reservoir locations in the area.

Acknowledgments

We thank the Faculty of Engineering, the University of Lampung, which has funded this research to complete this article.

References

[1] Sudarman S, Suroto, Pudyastuti K, and Aspiyo S 2000 *Proc. World Geotherm. Congr. 2000* 455
[2] Hochstein M P and Sudarman S 2008 *Geothermics* **37** 220
[3] Saefulhak Y 2017 *Potensi Panas Bumi Indonesia Jilid 1* (Jakarta: Direktorat Panas Bumi Direktorat Jenderal Energi Baru, Terbarukan dan Konservasi Energi Kementerian Energi dan Sumber Daya Mineral)
[4] Zaenudin A, Karyanto, Damayanti L, and Sarkowi M 2011 *11th Annu. Indones. Geotherm. Assoc. Meet. Conf.* 324
[5] Haerudin N, Karyanto, and Kuntoro Y 2016 *Asian Res. Publ. Netw. J. Eng. Appl. Sci.* **11** 4804
[6] Taufiq 2020 *IOP Conf. Ser. Mater. Sci. Eng*. **982** 012049
[7] Karyanto, Haerudin N, Mulyasari R, Suharno, and Manurung P 2020 *J. Earth Space Phys*. **45** 98
[8] Mangga SA, Amirudin, Suwarti T, Gafoer S, Sidarta 1993 *Peta Geologi Lembar Tanjungkarang, Sumatera, skala 1:250.000* (Jakarta: Perpusatakaan Nasional Indonesia)
[9] Anonym 2021 *Extract XYZ Grid - Topography or Gravity* Retrived from: https://topex.ucsd.edu/cgi-bin/get_data.cgi
[10] Blakely R J 1995 *Potential Theory in Gravity and Magnetic Applications* (Cambridge: Cambridge University Press)
[11] Al-Khafaji W M S 2017 *Baghdad Sci. J.* **14** 625
[12] Ming Y, Niu X, Xie X, Han Z, Li Q, and Sun S 2021 *IOP Conf. Ser. Earth Environ. Sci.* **660** 012057
[13] Sumintadireja P, Dahrin D, and Grandis H 2018 *J. Eng. Technol. Sci*. **50** 127
[14] Muhammad Y, Faisal A, Yenny A, Muzakir Z, Abubakar M, and Nazli I 2021 *J. Teknol.* **83** 145
[15] Elkins T A 1951 *Geophys.* **16** 29
[16] Sarkowi M and Wibowo R C 2021 *J. Appl. Sci. Eng*. **25** 392
[17] Witter J B, Stelling P, Knapp P, and Hinz N H 2016 *Geotherm. Resour. Counc. Trans.* **40** 647
[18] Rosid M S and Sibarani C 2021 *J. Phys. Conf. Ser.* **1816** 012083

[19] Department of Earth and Ocean Science 2005 *GRAV3D Version 2.0 A Program Library for Forward Modelling and Inversion of Gravity Data over 3D Structures* (Columbia: University of British Columbia)
[20] Cevallos C 2018 *Geophys.* **82** G115
[21] Sarkowi M 2010 *J. Sains MIPA* **16** 111
[22] Plouff D 1976 *Geophys.* **41** 727
[23] Hafidah AD, Daud Y, and Usman A 2019 *E3S Web Conf*. **125** 14008
[24] Daud Y, Rosid M S, Pati G P, Maulana M R, and Khoiroh M 2018 *AIP Conf. Proc.* **2023** 020263
[25] Puspita O D, Juniarto R, Larasati S S, Hamdalah H, and Takodama I 2020 *J. Phys. Sci. Eng*. **5** 22
[26] Suryadi, Haerudin N, Karyanto, and Sudrajat Y 2019 *J. Geofis. Eksplor*. **3** 85
[27] Maithya J, Fujimitsu Y, and Nishijima J 2020 *Geothermics* **85** 101795
[28] Siratovich P A, Heap M J, Villenueve M C, and Cole J W Reuschle T 2014 *Geotherm. Energy* **2** 10